frontiers | Frontiers in Earth Science

TYPE Original Research
PUBLISHED 02 July 2025
DOI 10.3389/feart.2025.1627767

OPEN ACCESS

EDITED BY
Jingbin Wang,
SINOPEC Petroleum Exploration and Production Research Institute, China

REVIEWED BY
Chao Yang,
Chinese Academy of Sciences (CAS), China
Lian Jiang,
Macquarie University, Australia

*CORRESPONDENCE
Hou Dujie,
hdj@cugb.edu.cn

RECEIVED 13 May 2025
ACCEPTED 16 June 2025
PUBLISHED 02 July 2025

CITATION
Yuhan J, Ruibo G, Dujie H and Xiong C (2025) Classification of crude oil and its correlation with terrestrial plant inputs across different areas in the Xihu Depression, East China Sea Shelf basin: insights from organic geochemical evidence.
Front. Earth Sci. 13:1627767.
doi: 10.3389/feart.2025.1627767

Classification of crude oil and its correlation with terrestrial plant inputs across different areas in the Xihu Depression, East China Sea Shelf basin: insights from organic geochemical evidence

Jiang Yuhan[1,2], Guo Ruibo[3], Hou Dujie[2]* and Cheng Xiong[2]

[1]Key Laboratory of Marine Mineral Resources, Ministry of Natural Resources, Guangzhou Marine Geological Survey, China Geological Survey, Guangzhou, China, [2]School of Energy Resources, China University of Geosciences, Beijing, China, [3]National Engineering Research Center of Gas Hydrate Exploration and Development, Guangzhou Marine Geological Survey, Guangzhou, China

Introduction: While crude oils in the Xihu Depression are known to originate from terrestrial sources, a systematic classification linking their geochemistry to specific plant inputs has been lacking. This study utilizes detailed organic geochemistry to classify these oils and elucidate the relationship between their composition, source, and depositional environment.

Methods: Using gas chromatography-mass spectrometry (GC-MS), we analyzed saturate and aromatic fractions of 41 crude oils from the Xihu Depression, then applied multivariate statistical analysis to classify them based on key biomarker parameters.

Results and discussion: The results indicate that the oils are enriched in biomarkers reflecting substantial contributions from terrestrial higher plants, particularly tricyclic diterpanes and their aromatized derivatives originating from angiosperms, gymnosperms, and ferns. In contrast, biomarkers indicative of contributions from aquatic lower organisms were present in relatively low concentrations. Significant variations in the composition of these biomarkers across different structural zones were observed. Statistical analysis of these compositional differences allowed for the classification of the crude oils into four distinct groups. The four categories reflect varying inputs from ferns, gymnosperms, and angiosperms. A new (isopimarane+1,7-DMP)/(16β(H)phyllocladane+retene), effectively assesses gymnosperm versus fern inputs. Higher values of this index indicate a greater gymnosperm contribution. A positive correlation between this index and δ13Coil values highlights the pivotal role of gymnosperm resins in hydrocarbon generation within the Xihu Depression.

KEYWORDS

biomarkers, organic matter source, organic geochemistry, diterpanes, oil classification

1 Introduction

Coal-bearing source rocks constitute one of the principal contributors to liquid hydrocarbons in many Meso-/Cenozoic basins. Giant oil and gas accumulations sourced from such strata have been reported in the Gippsland, Kutai, Malay, Tuha, Barito, Gongola, Greater Green River and Guasare basins, among others (GarcíaGonzález et al., 1997; Obaje and Hamza, 2000; Jauro et al., 2007; Abbassi et al., 2016; Escobar et al., 2016; Ayinla et al., 2017). Beyond their economic importance, the study of coal-derived oils offers profound insights into both Earth's history and energy resources. These oils not only preserve detailed records of palaeovegetation evolution and palaeoclimatic conditions, but systematic analysis of their compositional variations, especially those linked to specific terrestrial higher plant precursors, provides a powerful tool for identifying favourable petroleum systems and understanding the intricate interplay of factors governing organic matter accumulation in ancient coastal environments.

The Xihu Depression, a major Cenozoic petroliferous depression in the East China Sea Basin, represents a prime example where oil and gas reserves are predominantly sourced from Paleogene coal-bearing sequences, specifically the Eocene Pinghu Formation deposited in a coastal marsh environment (Shen et al., 2016; Cheng et al., 2019; Kang et al., 2020; Yang et al., 2023). These source rocks, encompassing coal, carbonaceous mudstone, and mudstone with Type II and Type III kerogen and high TOC (up to 75.68%), exhibit significant hydrocarbon generation potential (Su et al., 2019; Zhu et al., 2020; Wang et al., 2020a; Quan et al., 2022). However, the heterogeneity of these source rocks and depositional facies, coupled with challenges in obtaining extensive core data due to offshore drilling costs, has led to ongoing discussions regarding the precise contributions of different lithologies and terrestrial organic matter types to the accumulated hydrocarbons (Ye et al., 2007; Xie et al., 2018; Cheng et al., 2020a; Wang et al., 2020b; Li et al., 2023). Previous geochemical studies have characterized oils from the Xihu Depression, generally confirming their origin from the Pinghu Formation source rocks and identifying the presence of terrestrial biomarkers (Su et al., 2013; Xu et al., 2016; Cao et al., 2019; Zhu, 2020; Cheng et al., 2020b). Nonetheless, significant variations in oil properties and geochemical compositions are observed across different structural zones within the Depression (e.g., central trough vs. slope breaks), implying variations in source input, maturity, or alteration effects that are not yet fully understood (Xu et al., 2016; Zhu et al., 2021).

While a broad terrestrial higher plant origin is recognized, the precise nature and differential contributions of specific biogenic precursors responsible for these variations remain inadequately constrained. Specifically, a systematic classification of these oils based on detailed molecular geochemistry, which would be crucial for integrating information from both aliphatic and aromatic fractions to clearly link oil characteristics to specific terrestrial plant inputs (e.g., angiosperm vs. gymnosperm contributions) and subtle depositional environmental shifts (e.g., salinity, redox conditions) across different tectonic settings, remains underdeveloped. This lack of detailed characterization underscores the necessity, as noted by previous researchers (e.g., Su et al., 2013; Zhu et al., 2021), for a more comprehensive analysis to unravel the paleogeographic information and origins of different oil types within the basin.

To address this gap, this study undertakes a detailed organic geochemical investigation of 41 crude oil samples collected from various structural zones across the Xihu Depression. We analyze both aliphatic and aromatic hydrocarbon fractions using gas chromatography-mass spectrometry (GC-MS), focusing on a wide range of biomarker compounds indicative of organic matter source, depositional environment, and thermal maturity. A key objective and novelty of this work is to leverage the integrated dataset, particularly the distribution of terrigenous biomarkers such as diterpenoids (aliphatic) and their potential aromatic derivatives (e.g., phenanthrenes, naphthalenes), to explore new geochemical indices. These indices aim to differentiate subtle variations in higher plant inputs and depositional conditions more effectively. By systematically classifying the oils and correlating their geochemical fingerprints with inferred paleo-inputs and geological settings, this research seeks to: (1) establish a refined geochemical framework that delineates distinct oil families within the Xihu Depression, directly linking their compositional heterogeneity to variations in terrestrial organic matter contributions across different structural units; (2) develop and validate novel biomarker-based indices to more precisely quantify the relative inputs from specific higher plant precursors, thereby enhancing our ability to trace oil origins and understand source-specific imprints; and (3) ultimately, enhance the understanding of the Xihu Depression's petroleum system by elucidating the significant role of diverse terrestrial floras in hydrocarbon generation, and provide valuable, scientifically-grounded insights for future hydrocarbon exploration and oil quality prediction in this significant basin.

2 Geology setting

Xihu Depression, located in the central part of the mid-eastern fault zone of the East China Sea Shelf Basin (ECSSB), is a significant Mesozoic and Cenozoic oil- and gas-bearing depression within the basin. It extends over 480 km from north to south and has a width of 70–130 km from east to west, encompassing an area of approximately 51,800 km^2. The depression is geographically divided from west to east into the western slope area, the central sag, and the eastern boundary fault zone. The western slope area is further subdivided from north to south into the Kongqueting (KQT), Wuyingting-Baoyunting (WYT-BYT), and Tuanjieting-Pinghu (TJT-PH) structural zones; the central sag consists of the west minor sag (WMS) in the west, and to the east, in a north-south arrangement, it includes the Jiaxing (outside the study area), Ningbo (NB), Huangyan (HY), and Tiantai (TT) structural zones (Figure 1). Previous research has yielded systematic stratigraphic analyses of the ECSSB, uncovering a multitude of microfossil zones (Qin et al., 1998; Wu, 2014) or assemblages and constructing a stratigraphic sequence and chronostratigraphic framework for the basin (Zhu et al., 2012; Zhang et al., 2015; Zhao et al., 2016). Within Xihu Depression, the Cenozoic sedimentary thickness surpasses 20,000 m, with rifting initiating in the Late Cretaceous and sedimentary infilling persisting into the Paleocene-Eocene epochs (Yang et al., 2011; Zhang and Jiang, 2013; Abbas et al., 2018; He et al., 2023). The crude oil samples analyzed in this research are primarily from the Upper Eocene Pinghu Formation and the Oligocene Huagang Formation.

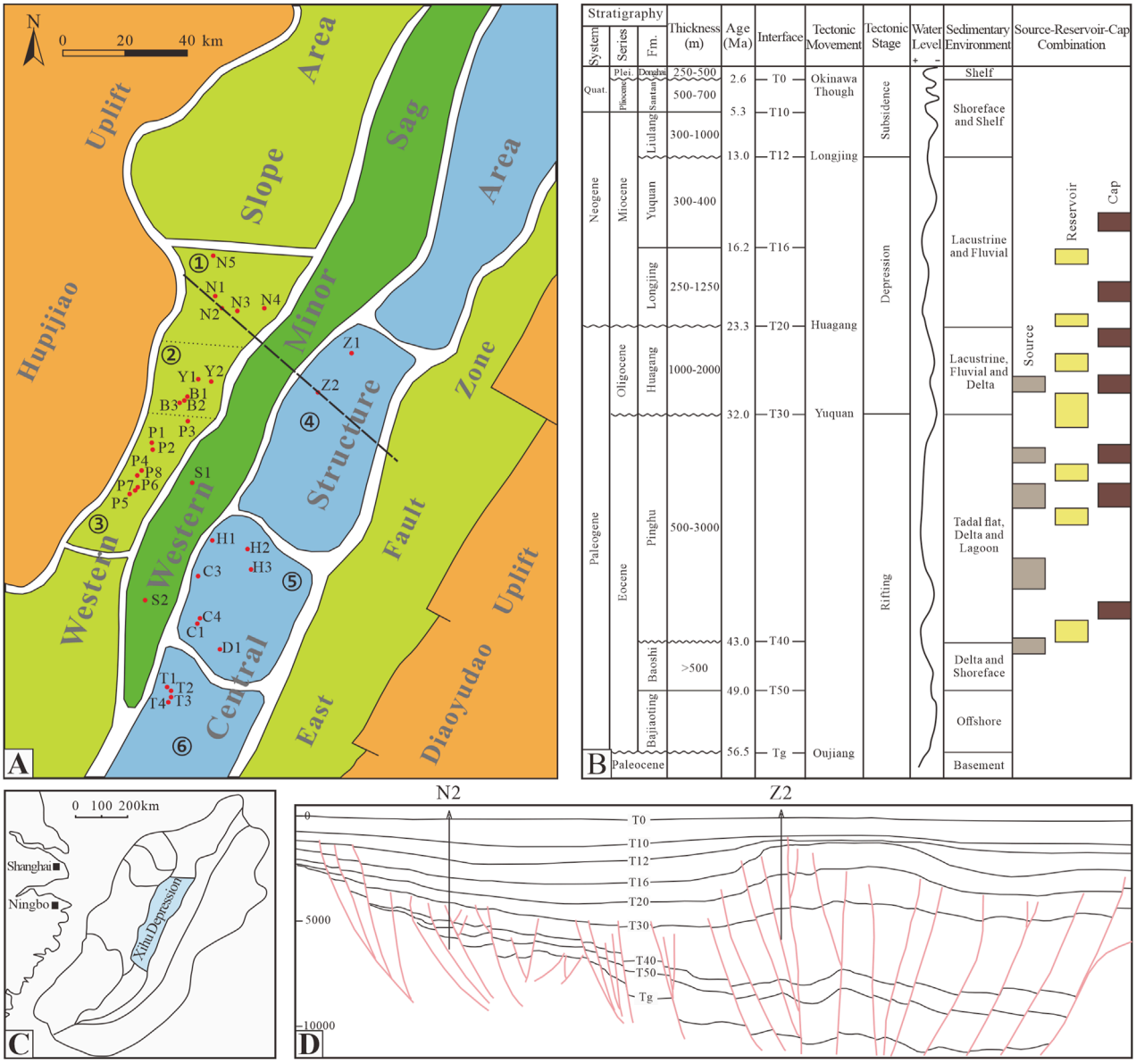

FIGURE 1
(A) Planar distribution map of structural zones and well locations in the study area (red dot, well location; ① KQT structural zone; ② WYT-BYT structural zone; ③ TJT-PH structural zone; ④ NB structural zone; ⑤ HY structural zone; ⑥ TT structural zone; the black dashed line, the location of section in the Panel **(D)**). **(B)** Comprehensive stratigraphic column of the Xihu Depression (modified from Wei, 2013; Wang et al., 2022). **(C)** Geographic location of the Xihu Depression (light blue area). **(D)** Typical NW-SE seismic stratigraphic profile of the Xihu Depression.

3 Materials and methods

A total of 41 crude oil samples were obtained for this study from the Shanghai Branch of the China National Offshore Oil Corporation (CNOOC). Sample selection aimed to achieve broad representativeness of the petroleum characteristics within the Xihu Depression. Accordingly, the samples were collected from nearly all major structural zones and key reservior intervals within the depression. Specifically, based on sampling stratigraphy, 20 samples were sourced from the Huagang Formation and 21 samples from the Pinghu Formation. Geographically, the samples cover seven major structural zones: KQT (n = 8), WYT-BYT (n = 6), TJT-PH (n = 10), WMS (n = 3), NB (n = 3), HY (n = 7), and TT (n = 4). Each sample was preserved in a brown glass bottle, that had been pre-cleaned with trichloromethane.

A detailed analytical assessment was performed on the samples, encompassing aliphatic hydrocarbon gas chromatography (GC) and gas chromatography-mass spectrometry (GC-MS). The GC analyses utilized an Agilent 7890 A system equipped with an HP-1 fused-silica capillary column (60 m × 0.25 mm × 0.25 μm). The temperature program commenced at an initial temperature of 40°C, maintained for 10 min, followed by an increment of 4 C/min to 70°C, and then 8°C/min to a final temperature of 300°C, which was sustained for 40 min. For GC-MS, an Agilent 7890A-5975C with an

HP-5MS fused-silica capillary column (30 m × 0.25 mm × 0.25 μm) was employed; the temperature program initiated at 50°C, held for 1 min, with a subsequent rise of 20 C/min to 120°C, then 3 C/min to 310°C, which was maintained for 15 min. These studies were conducted at the Beijing Key Laboratory of Unconventional Natural Gas Geology Evaluation and Development Engineering, affiliated with the China University of Geosciences (Beijing).

In addition to the GC and GC-MS analyses conducted for this study, the Shanghai Branch of CNOOC provided a broader range of complementary geochemical data, which included the data for the 41 oil samples analyzed in this work. This dataset provided by CNOOC included bulk physical properties, carbon isotope ratios ($\delta^{13}C$ of whole oil, aliphatic and aromatic fractions), and bulk fraction chromatographic data (GC of aliphatic and aromatic hydrocarbons). The integration of these datasets allows for a comprehensive characterization of the oil samples.

4 Results

4.1 Crude oil physical properties and $\delta^{13}C$ characteristics

The crude oils within the Xihu Depression exhibit characteristics of condensates to light oils with a low-density spectrum, spanning from 0.74 to 0.90 g cm^{-3}, averaging at 0.81 g cm^{-3} (Table 1). The pour point of most samples falls between −20°C and 20°C, signifying a classification of low to medium pour point oils (Table 1). The kinematic viscosity of the crude oil samples varies from 0.16 to 12.59 mm^2 s^{-1}, averaging at 1.85 mm^2 s^{-1}, predominantly categorized as extra low to low viscosity oils (Table 1). The sulfur content in the Xihu Depression's crude oils is typically low, with an average of merely 0.08% (Table 1). Conversely, the wax content in the crude oil samples ranges from 0.00% to 26.81%, encompassing both low wax and high wax crude oils (Table 1). Notably, the wax content in the TJT-PH, WYT-BYT, and WMS crude oils is markedly higher than in other areas, and high wax crude oils frequently derive from the middle strata of the Pinghu Formation (E_2p^{3-4}; Figure 2). Given that the wax in crude oil predominantly originates from terrestrial plants, including plant waxes, cuticles, and spores, the presence of high wax crude oils in specific areas and layers suggests a unique organic matter source input for these oils.

Compared to crude oils from other rift lake basins in eastern China, those from the Xihu Depression exhibit relatively heavier carbon isotopic compositions. The $\delta^{13}C_{oil}$ values of crude oils in the Xihu Depression range from −24.8 to −27.6‰, predominantly clustering between −26.0 and −27.1‰. The $\delta^{13}C_{aliphatic}$ values range from −25.7 to −28.7‰, primarily distributed between −26.7 and −28.0‰. The $\delta^{13}C_{aromatics}$ values range from −24.6 to −26.6‰, with most samples falling between −24.8 and −26.5‰ (Supplementary Table S1).

Slight regional differences are observed in the $\delta^{13}C$ of the crude oils. Specifically, crude oil samples from the western slope area exhibit heavier $\delta^{13}C_{oil}$ and $\delta^{13}C_{aliphatic}$ values compared to those from the central structural area, whereas the $\delta^{13}C_{aromatics}$ values show little variation between these two areas (Figure 3). Although the bulk carbon isotope values may not be sufficient to fully differentiate the source materials of the crude oils, they nonetheless suggest a certain diversity in organic matter sources within the study area.

4.2 Aliphatic hydrocarbon characteristics of the crude oil

4.2.1 *n*-Alkanes and acyclic isoprenoids

In the crude oils from the Xihu Depression, the distribution of *n*-alkanes spans from nC_9 to nC_{33}, displaying a unimodal pattern with the primary peak generally located between nC_9 and nC_{14} (Supplementary Figure S1). These oils are characterized by a high concentration of low carbon number compounds and a relatively low abundance of high carbon number compounds, a feature that contrasts with the typical higher plant organic matter source input. This inconsistency is due to the modification of the crude oils by evaporative fractionation. As depicted in the plot of the logarithm of molar concentrations of *n*-alkanes versus carbon number (Figure 4), the concentrations of low carbon number *n*-alkanes (nC_9 to nC_{15}) are elevated in the crude oils from the study area, whereas those of medium to high carbon number *n*-alkanes (nC_{16} to nC_{39}) are diminished, exhibiting a two-segment distribution that markedly differs from the near-linear distribution typical of normal crude oils. This pattern is indicative of the influence of evaporative fractionation (Losh et al., 2002; He et al., 2023).

The Pr/Ph ratios of the crude oils in the study area consistently exceed 5, with the highest value reaching 13.11, and are predominantly concentrated between 6 and 9 (Supplementary Table S1). This distribution indicates a pronounced oxidative environment with significant input of higher terrestrial organic matter. As shown in Figure 5, the crude oils from the Xihu Depression display elevated Pr/nC_{17} ratios and reduced Ph/nC_{18} ratios, suggesting the input of terrigenous type III organic matter under oxidative conditions.

4.2.2 Diterpenoids

Crude oil samples from the Xihu Depression are characterized by an unusually rich assemblage of diterpanes, including bicyclic, tricyclic, and tetracyclic compounds, which are prevalent in coal-bearing source rocks and serve as crucial biomarkers for the identification and differentiation of petroleum derived from coal-bearing source rocks (Xu et al., 2015). In certain samples, the abundance of these diterpanes is almost equal to that of the adjacent *n*-alkanes as observed on the gas chromatograms (Supplementary Figure S1, between nC_{19} and nC_{21}).

Building upon previous research (Fu, 1994; Zhu et al., 2012), this study used the *m/z* 123 mass chromatogram to identify 13 diterpanes in the crude oils (Figure 6). These include bicyclic 8β(H)-labdane, tricyclic norisopimarane, 4β(H)-19-norisopimarane, fichtelite, rimuane, pimarane, isopimarane, and tetracyclic 16β(H)-phyllocladane, 16α(H)-phyllocladane, along with two unnamed C_{20} tetracyclic diterpanes. Notably, 4β(H)-19-norisopimarane, isopimarane, and 16β(H)-phyllocladane are the most abundant. However, beyerane and kaurane were not detected in the samples, despite previous studies erroneously identifying peak 11 (16α(H)-phyllocladane) as 16β(H)-kaurane.

TABLE 1 Physical property statistics of crude oil samples from different structures.

Structure	Density/g·cm^{-3}	Solidifying point/°C	Viscosity/mm^2·s^{-1}	Sulfur/%	Wax/%
TJT-PH	0.77~0.87 (46)/0.82	−57~29 (46)/2.04	1.03~5.22 (42)/2.03	0.01~0.42 (44)/0.06	0.09~19.53 (45)/5.11
WYT-BYT	0.82~0.90 (17)/0.85	−84~37 (17)/7.35	1.14~12.59 (16)/3.35	0.02~0.35 (15)/0.11	0.70~26.81 (16)/13.04
KQT	0.76~0.83 (9)/0.78	−36~2 (9)/-17.67	0.54~4.73 (9)/1.78	0.02~0.76 (8)/0.17	0.04~5.95 (8)/1.22
WMS	0.80~0.87 (11)/0.83	−9~27 (11)/11.82	0.16~12.59 (10)/1.85	0.00~0.76 (10)/0.08	0.00~26.81 (11)/5.28
TT	0.76~0.79 (21)/0.78	−25~19 (21)/-8.33	0.46~2.48 (21)/1.09	0.00~0.65 (16)/0.09	0.26~7.33 (14)/1.58
HY	0.74~0.78 (14)/0.82	−55~1 (14)/-22.79	0.16~2.15 (14)/1.09	0.00~0.32 (10)/0.10	0.00~2.70 (13)/0.77
NB	0.77~0.78 (4)/0.78	−14~2 (4)/-6.50	0.84~1.10 (4)/0.97	0.03~0.17 (3)/0.08	0.79~3.81 (4)/2.51

Notes: minimum~maximum (count)/average.

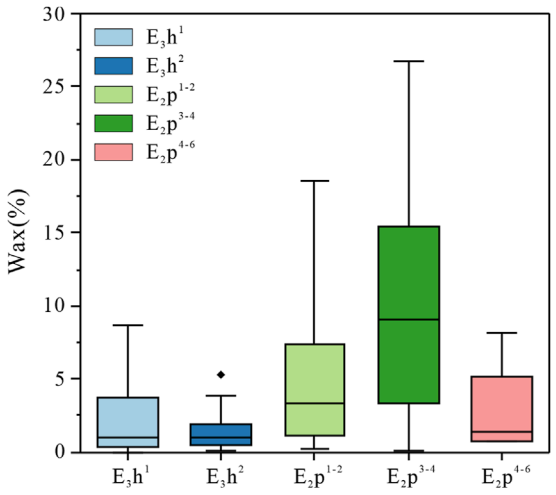

FIGURE 2
Box diagram of the wax content of oil samples from different strata, showing that samples from the Pinghu Formation contain more wax than those from the overlying Huagang Formation.

The abundance of diterpanes in crude oils from various structural zones within the Xihu Depression exhibits notable variability (Figure 7; Supplementary Table S2). In particular, the crude oils from the WYT-BYT and KQT region in the northern part of the western slope area demonstrate significantly higher diterpanes concentrations compared to other structural zones. The variation in the diterpanes/nC$_{20}$ ratios across different areas indicates a predominant contribution of higher plant resins, which are rich in diterpanes, to hydrocarbon generation on the northern part of western slope area. However, it is important to note that the crude oil from well N1 and those from the NB structural zone display lower diterpanes abundances due to the effects of thermal evolution (R$_c$ = 1.57). Previous research (Baset et al., 1980; Hou et al., 1992; Jiang et al., 2020) has demonstrated that excessive maturity often leads to the decomposition of diterpanes.

Despite the significant variations in diterpane abundance among different samples, there is a certain similarity in their distribution patterns. Among the 41 samples tested, except for five samples from wells D1, T1, T3, and T4, which exhibit a distribution pattern of 16β(H)-phyllocladane > isopimarane ≈ 4β(H)-19-norisopimarane, all other samples show a distribution pattern of either isopimarane > 4β(H)-19-norisopimarane > 16β(H)-phyllocladane or 4β(H)-19-norisopimarane > isopimarane > 16β(H)-phyllocladane. The isopimarane/(isopimarane + 16β(H)-phyllocladane) parameter generally shows higher values in the northern regions and lower values in the southern regions. Both the isopimarane/nC$_{20}$ and isopimarane/(isopimarane +16β(H)-phyllocladane) ratios reflect differences in the quantity and type of diterpanes precursor substances across different regions, which may be key factors determining the geochemical characteristics of crude oils in the Xihu Depression.

4.2.3 Pentacyclic triterpanes and steranes

The Ts/Tm ratio in samples from the Xihu Depression is generally very low, with an average value of only 0.31, which is significantly lower than that of typical mature crude oils. This low ratio may be attributed to limited clay-catalyzed reactions in coal-bearing formations (Keshirtsev et al., 2010; Zhang and Zhang, 2012). Within the hopane series, C$_{30}$ hopane is predominant, and C$_{29}$ hopane also exhibits relatively high abundance. However, the abundance of hopane homologues markedly decreases with increasing carbon number, with C$_{33}$, C$_{34}$, and C$_{35}$ hopanes being either extremely low or undetectable (Supplementary Figure S2), reflecting an oxidizing depositional environment.

Sterane compounds could be identified in only a few samples. Most samples exhibit a regular sterane distribution pattern resembling an “inverted L” shape, while a few exhibit a “V” shape (Supplementary Figure S2), with C$_{29}$ regular steranes being predominant. Overall, this indicates that the crude oil is derived from higher plants. Notably, the samples contain abundant C$_{29}$ diasteranes, which often co-elute with C$_{27}$ regular steranes in the m/z 217 mass chromatogram, thereby interfering with the qualitative and quantitative analysis of C$_{27}$ regular steranes. Consequently, the seemingly high content of C$_{27}$ regular steranes in some samples may not be reliable.

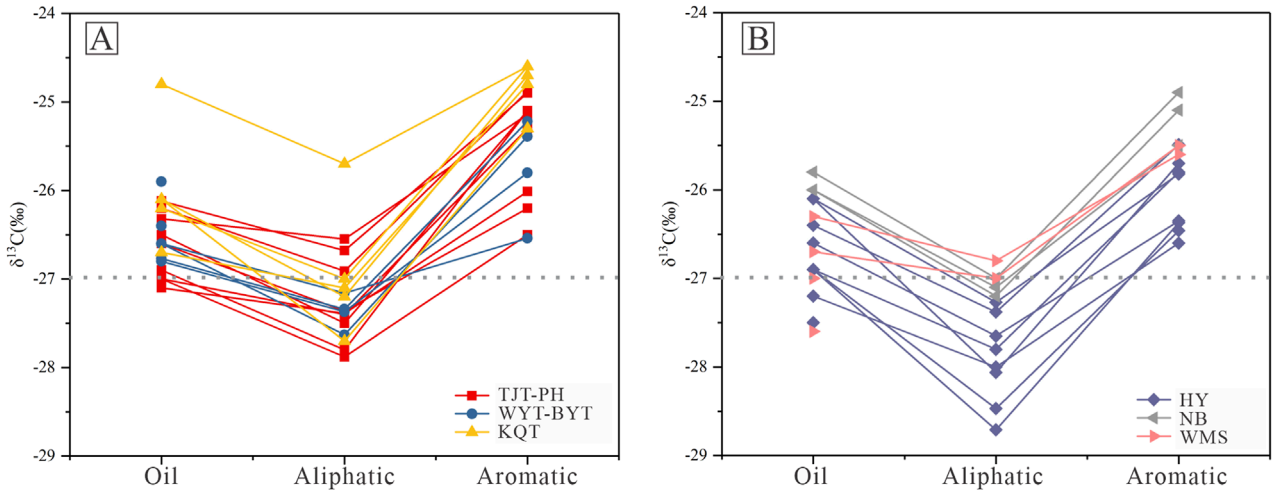

FIGURE 3
Stable carbon isotope ratio of oil samples from different structures in the Xihu Depression **(A)**, western slope; **(B)**, central sag. Using 27‰ as a reference (gray dashed line), the carbon isotope ratios of the western slope samples are higher than those of the central sag.

4.3 Aromatic hydrocarbon characteristics of the crude oil

Nine series and 151 types of compounds were identified in the aromatic hydrocarbons of crude oils from the Xihu Depression. After normalizing the abundance of these nine series of compounds, their relative contents were calculated, as shown in Figure 8. It is evident that the aromatic hydrocarbons in the crude oil from the Xihu Depression are predominantly composed of monocyclic short-chain alkylbenzene series, bicyclic naphthalene series and biphenyl series, and tricyclic phenanthrene series. The combined relative abundance of these four types of compounds exceeds 90%, reaching a maximum of 97.12%. Among these, the naphthalene series compounds have the highest abundance, accounting for more than 40% of the aromatic hydrocarbon content. The combined content of the dibenzofuran series, fluorene series, and dibenzothiophene series ranges from 2.73% to 8.46%, while the remaining chrysene series and benzo-naphtho-thiophene series have very low relative abundances, together accounting for only 0.05%–0.47%. The relatively high abundance of short-chain alkylbenzenes in the crude oil indicates potential bacterial origin contributions (Hartgers et al., 1994; Gorchs et al., 2003; Zhan et al., 2023) and the effects of evaporative fractionation (Thompson, 1988; Akinlua et al., 2006; Cai et al., 2009).

The aromatic composition of crude oil samples from the Xihu Depression exhibits certain differences among various structural zones. In the WYT-BYT and KQT areas on the northern part of the western slope, the content of the phenanthrene series in crude oil is significantly higher than in other areas, with an average abundance of 18.32%. The relative content of the phenanthrene series in the NB structural zone is also relatively high, at 7.03%. In contrast, the average content of the phenanthrene series in other structural zones is only 3.99% (Figure 8). Besides the phenanthrene series, the content of fluorene series compounds in crude oil samples from the WYT-BYT, KQT areas, and the NB structural zone is also slightly higher than in crude oil samples from other areas.

4.3.1 Naphthalene series compounds

In the crude oil samples from the Xihu Depression, a relatively complete series of naphthalene compounds can be identified in the *m/z* 128 + 132+156 + 170+184 + 198 mass chromatograms, including naphthalene, methyl-naphthalene (MN), dimethyl-naphthalene (DMN), trimethyl-naphthalene (TMN), tetramethyl-naphthalene (TeMN), and pentamethyl-naphthalene (PMN) series, with the naphthalene and methyl-naphthalene series being predominant (Supplementary Figure S3).

Alexander et al. (1985) and Zhao et al. (2013) suggested that 1,2,5-TMN and 1,2,5,6-TeMN are derived from pentacyclic triterpenoid amyrin or bicyclic diterpenoid sugiol from angiosperms, serving as indicators of terrestrial higher plant sources. The ratio of 1,2,5-TMN to 1,3,6-TMN in the tested samples ranges from 0.10 to 1.49, with an average of 0.52. The ratio of (1,2,5,6-TeMN +1,2,3,5-TeMN) to ∑TeMNs ranges from 0.03 to 0.34, with an average of 0.16. Both ratios exhibit abnormally high values in the TT structural zone, while being relatively similar in other areas, showing a slight trend of higher values in the south and lower values in the north (Supplementary Table S2). This suggests that the input of source materials in the TT structural zone might differ from other regions, and that there are also certain differences in the input of higher plants, represented by angiosperms, among the regions (Figure 9A). Regarding the stratigraphic units of the crude oil, the ratios are higher in the Huagang Formation than in the Pinghu Formation (Figure 9B), indicating an increasing trend of angiosperm input from the Pinghu Formation to the Huagang Formation in the Xihu Depression.

4.3.2 Phenanthrene series compounds

In the crude oil samples from the Xihu Depression, a relatively complete series of phenanthrene compounds can be identified in the *m/z* 198 + 192 + 206 + 220 +

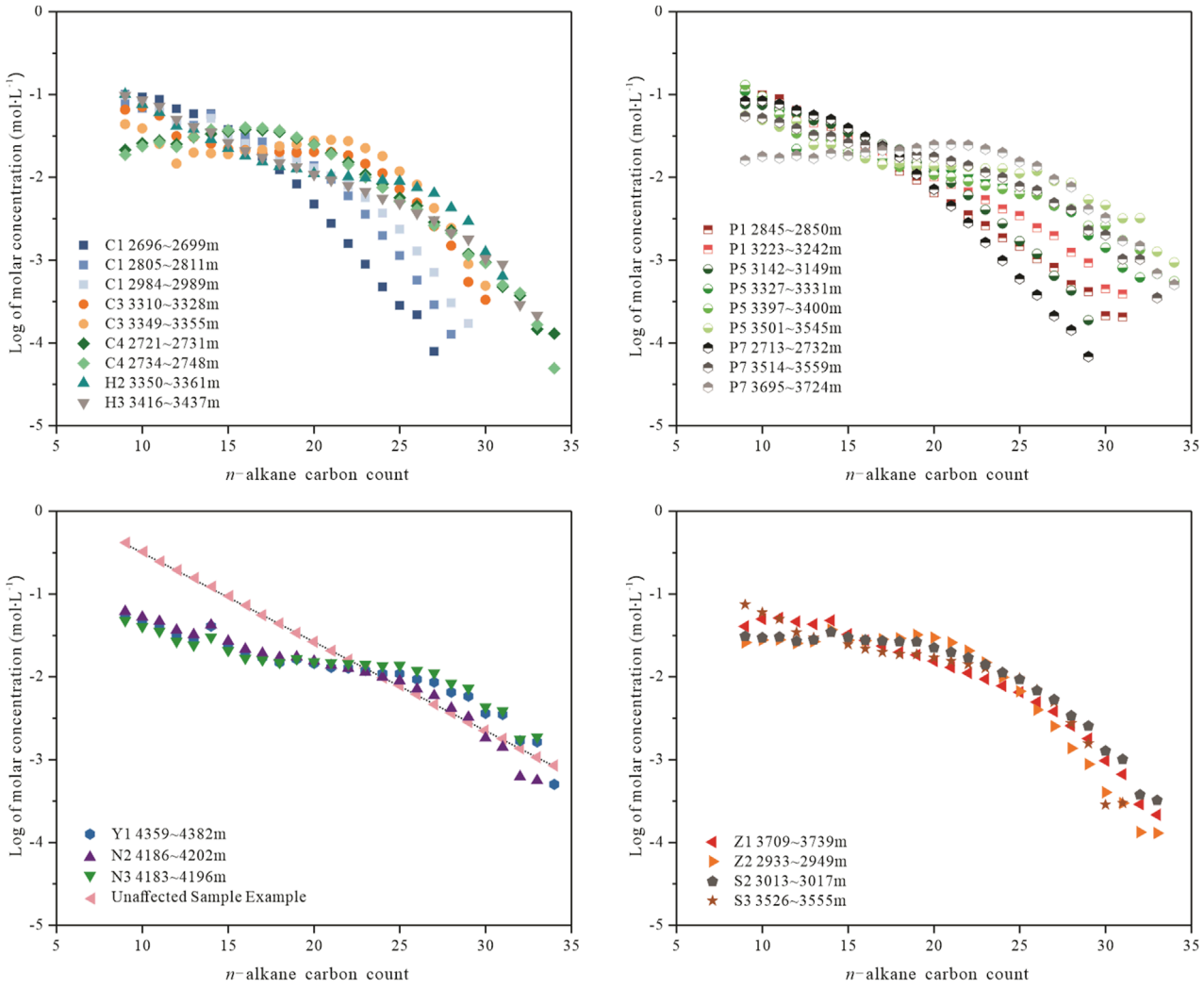

FIGURE 4
Log of molar concentration versus *n*-alkane carbon count of crude oil samples from different structures, suggesting the distribution of *n*-alkanes in samples from the study area is affected by the effect of evaporative partitioning.

234 mass chromatograms, including phenanthrene, methylphenanthrene (MP), dimethyl-phenanthrene (DMP), trimethylphenanthrene (TMP), and tetramethyl-phenanthrene (TeMP) series (Supplementary Figure S4). The mildly acidic coal-forming environment is conducive to the synthesis of certain unique alkylphenanthrene compounds (Le Metayer et al., 2014; Ding et al., 2022). The phenanthrene series compounds in the study area exhibit some "unusual" characteristics, such as a significantly higher abundance of 1-MP compared to 9-MP in certain samples; in some samples, the concentration of 1,7-DMP is close to or even exceeds that of phenanthrene. Most samples show an exceptionally high abundance of retene (7-isopropyl-1-methylphenanthrene), noticeably higher than other TeMP compounds in the *m/z* 234 mass chromatogram, with its concentration in some samples approaching that of MP compounds. Additionally, anthracene and 3-methylanthracene are also identified in many samples (Supplementary Figure S4). 1-MP and 1,7-DMP are aromatized diterpanes, indicating input from higher plants. Retene and anthracene are common markers of terrestrial higher plants often found in oxidized environments associated with coal-bearing strata (Budzinski et al., 1995; Zhu et al., 2012; Wu et al., 2024).

The 1-MP/9-MP ratio in the samples varies from 0.43 to 2.10, with an average of 1.14. The 1,7-DMP/phenanthrene ratio ranges from 0.08 to 3.51, with an average of 0.71. As illustrated in Figure 10 and Supplementary Table S2, the 1-MP/9-MP and 1,7-DMP/phenanthrene ratios in the western slope area (TJT-PH, WYT-BYT, and KQT structural zone) and WMS samples are higher than those in the central structural area samples (TT, HY, and NB structural zone). This indicates that the higher plant sources corresponding to 1-MP and 1,7-DMP contribute more significantly to the crude oil in the western slope areas of the Xihu Depression, especially in the WYT-BYT region. This is due to the fact that the slope areas have a richer abundance of coal-forming higher plants, and rivers bring in more plant debris compared to the central parts of the depression. The distribution characteristics of the

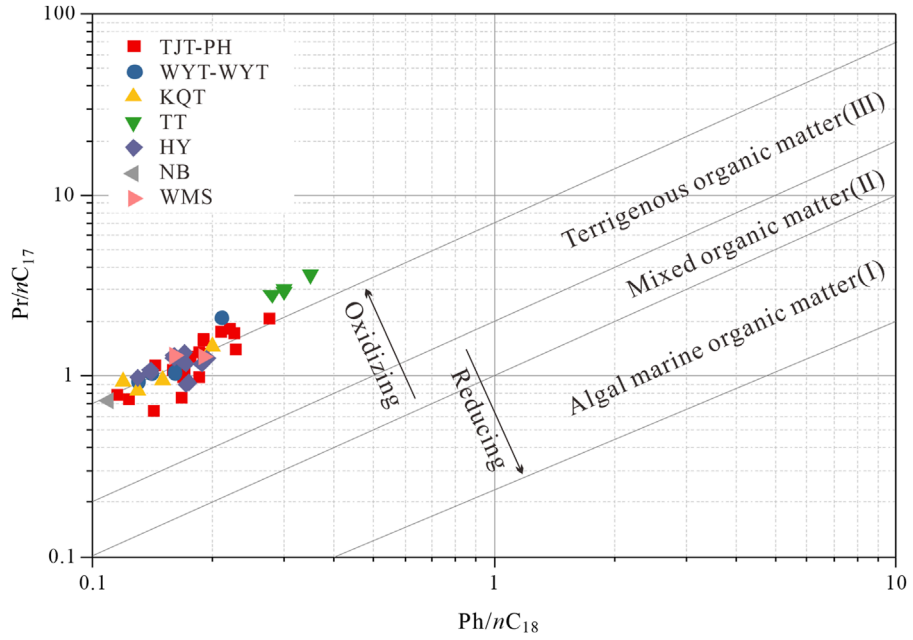

FIGURE 5
Plot of Ph/nC_{18} versus Pr/nC_{17}, showing that organic matter in the study area is type III organic matter, derived from oxidizing environments.

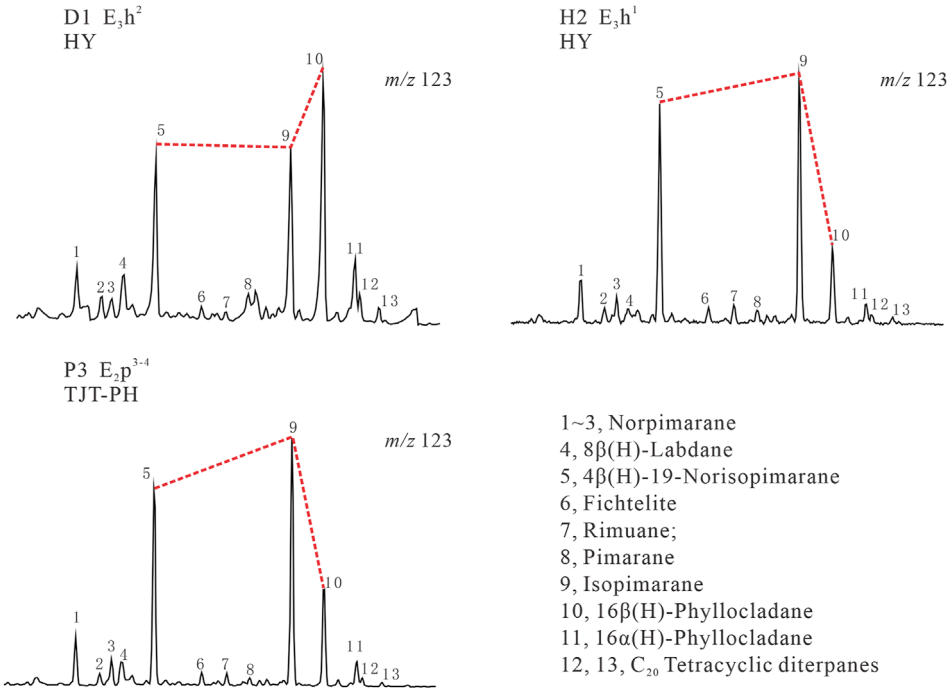

FIGURE 6
Diterpanes distribution of typical crude oil samples (*m/z* 123). There are primarily two different distribution patterns: one with peak 9 showing the highest abundance and the other with peak 10 showing the highest abundance.

aforementioned aromatic compounds in the crude oil from the Xihu Depression indicate that terrestrial coal-forming higher plants are the dominant source material, which is consistent with the indicators provided by the diterpanes biomarkers.

4.3.3 Fluorenes, dibenzofurans and dibenzothiophenes

Among the three series of compounds present in the crude oil samples from the Xihu Depression, the dibenzofurans exhibit

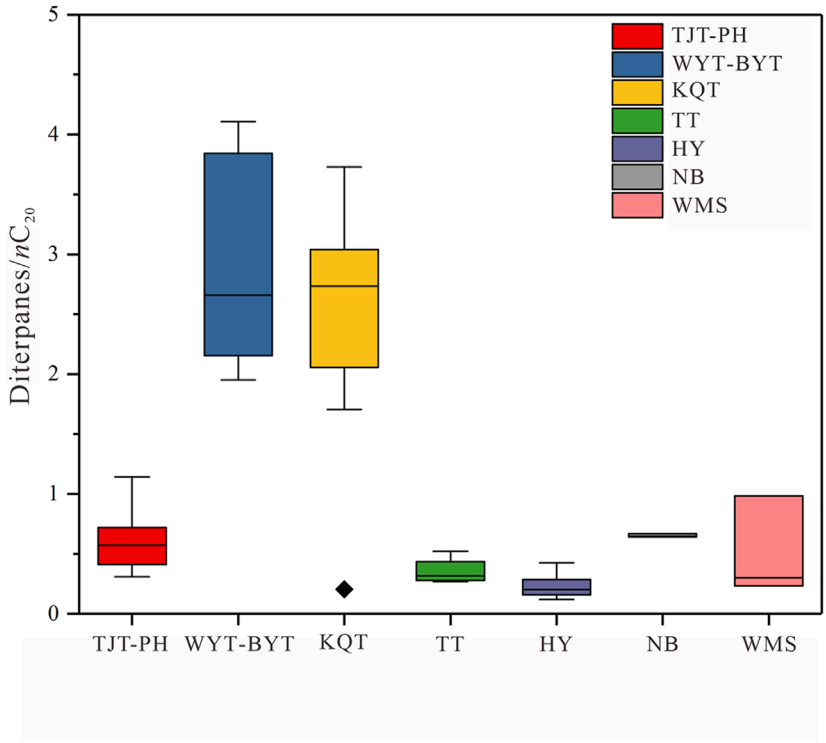

FIGURE 7
Diterpanes/nC_{20} ratio of crude oil samples in different structures. The content of diterpanes in the northern samples of the western slope (WYT-BYT and KQT) is significantly higher than that in the other areas.

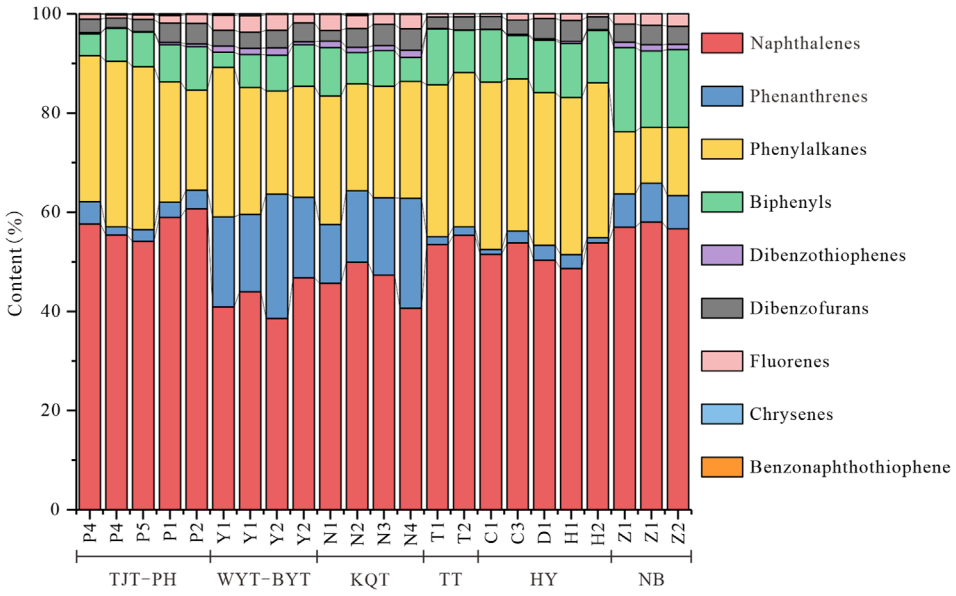

FIGURE 8
Weight percentage (Wt.%) of aromatic compounds in crude oil samples from different structures in the Xihu Depression. The relative content of phenanthrene series compounds in the northern samples of the western slope (WYT-BYT and KQT) is significantly higher than in the other areas.

the highest abundance, ranging from 32.42% to 85.80% (with an average of 61.96%, as shown in Supplementary Table S2). The fluorenes follow, with an abundance ranging from 8.95% to 48.24%, and an average of 29.14% (Supplementary Table S2). The dibenzothiophenes have a relatively lower abundance (0.91%–19.34%, with an average of 8.91%, Supplementary Table S2).

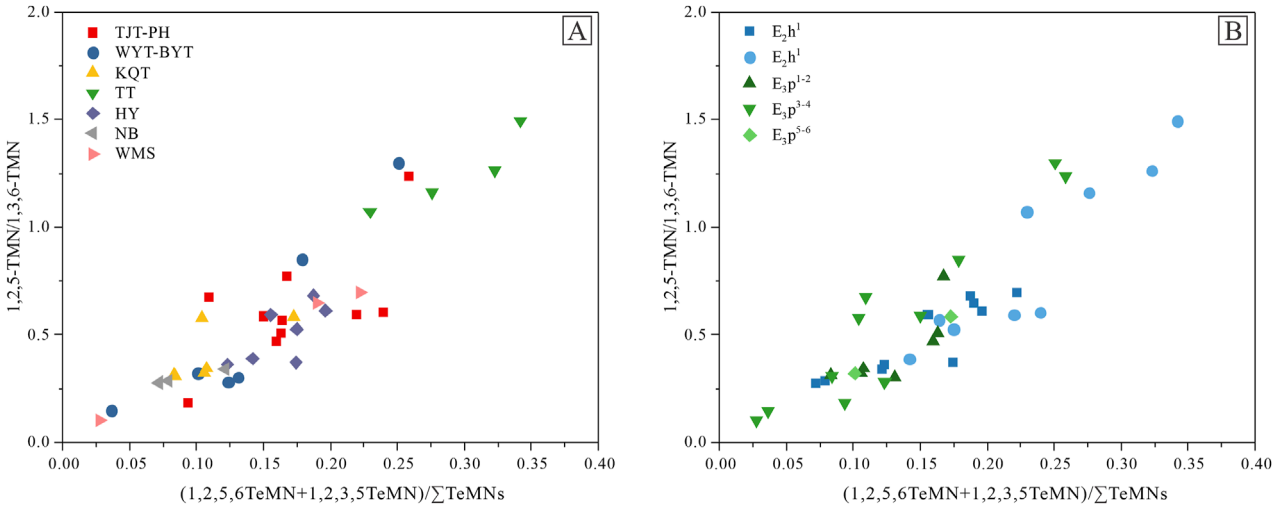

FIGURE 9
Correlation between 1,2,5-TMN/1,3,6-TMN and (1,2,5,6-TeMN + 1,2,3,5TeMN)/∑TeMNs of crude oil samples, classified by **(A)** structure and **(B)** stratum. The differences in these values between different structures and strata indicate variations in the plant sources of organic matter. Notes: TMN, trimethylnaphthalene; TeMN, tetramethylnaphthalene.

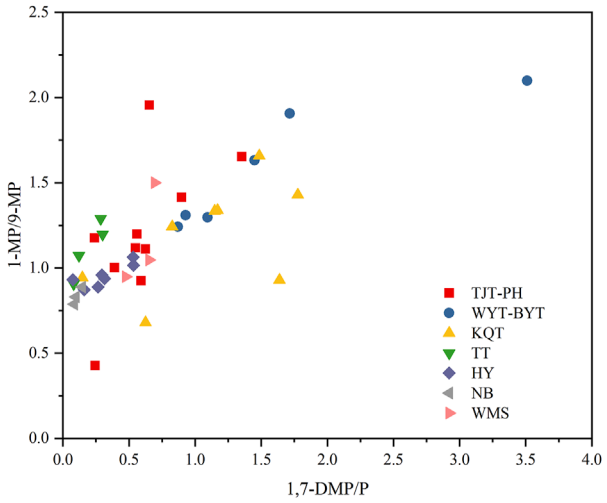

FIGURE 10
Correlation between 1-MP/9-MP and 1,7-DMP/P ratios of crude oil samples from different structures. The values of these two parameters in the northern sample of the western slope area are higher than those of the other areas. Notes: P, phenanthrene; MP, methyl-phenanthrene; DMP, dimethyl-phenanthrene.

The crude oils with higher abundances of the dibenzothiophene series are primarily derived from the WYT-BYT, KQT regions, and the NB structural zone. Overall, the composition of these three series of compounds in the crude oil from the Xihu Depression aligns with the characteristic high dibenzofuran and low dibenzothiophene content typically observed in coal-derived oils from swamp environments. Radke et al. (1991) proposed the use of the ratio of methyldibenzothiophene compounds to methyldibenzofuran compounds (MDBTs/MDBFs) in conjunction with Pr/Ph values as a means of determining the depositional environment of crude oil or organic matter. All samples are situated within the oxic environment of the fluvio/deltaic facies, as depicted in Supplementary Figure S5. However, the correlation between MDBTs/MDBFs and Pr/Ph is relatively weak.

5 Discussion

5.1 Classification of the crude oil families and categories

The experimental data indicate that the crude oil from the Xihu Depression is derived primarily from terrigenous organic matter deposited in an environment with a low degree of oxidation, resulting in the formation of light and condensate oils. However, significant variations exist in the geochemical characteristics of crude oils from different regions, necessitating their classification and the exploration of their respective origins. The depositional environment of the organic matter and the source input constitute important factors contributing to variations in the geochemical properties of petroleum and are thus pivotal for the classification of crude oil. In order to ensure analytical reliability and mitigate the influence of the previously discussed evaporative fractionation effects, this study constructs a series of parameters using compounds possessing relatively high concentrations of low to medium carbon numbers in the crude oil, rather than steranes and pentacyclic triterpane compounds, which are scarce and prone to analytical errors. The parameters employed include diterpanes/nC$_{20}$, Pr/nC$_{17}$, Ph/nC$_{18}$, Pr/Ph, diadrimane/8β(H)-drimane, 8β(H)-drimane/8β(H)-homodrimane, 4β(H)-19-nor-isopimarane/isopimarane, 16β(H)-phyllocladane/isopimarane, 1,2,5-trimethylnaphthalene/1,3,6-trimethylnaphthalene, 1,7-dimethyl-phenanthrene/phenanthrene, retene/phenanthrene, as well as the $\delta^{13}C_{oil}$.

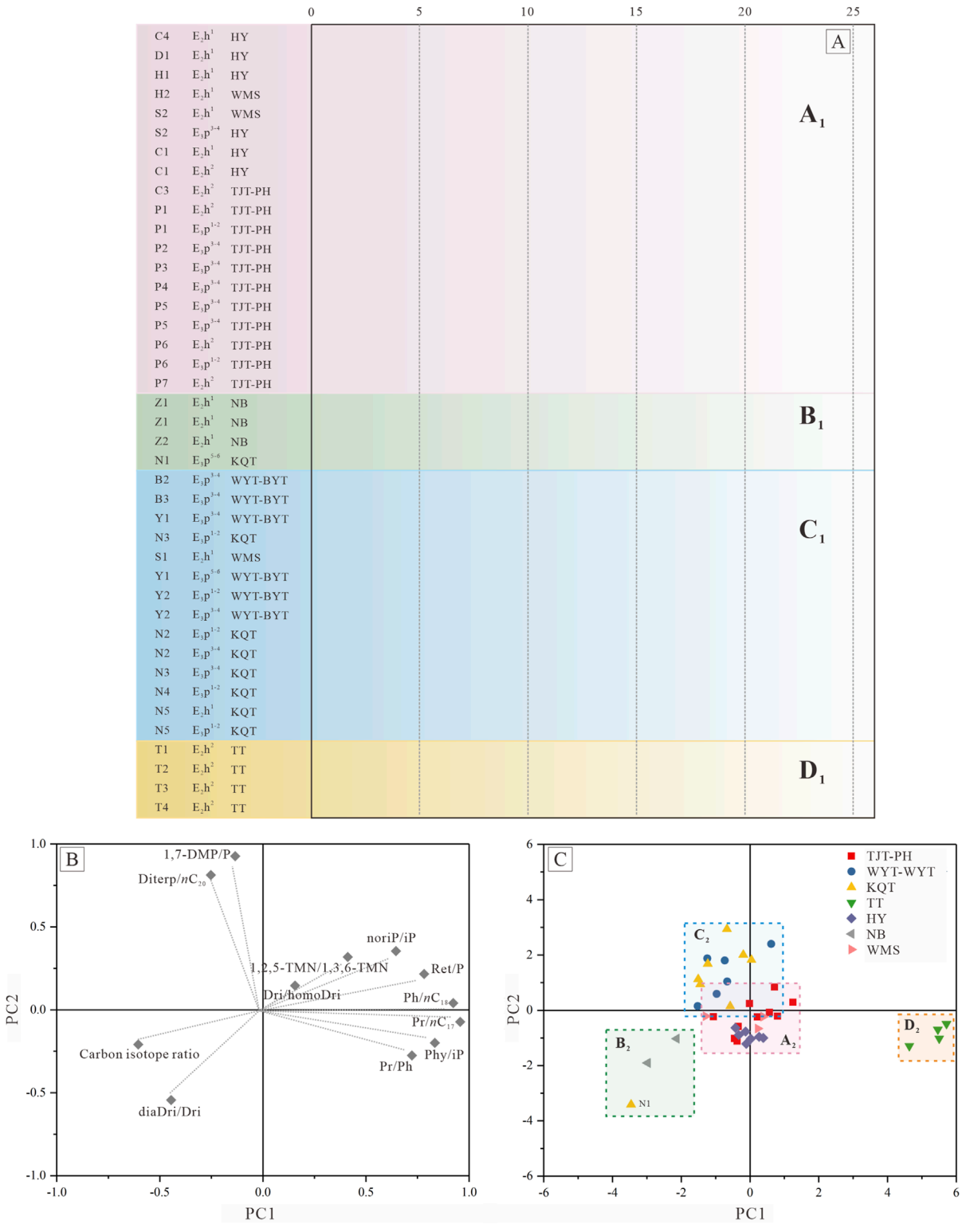

FIGURE 11
(A) Classification of crude oil samples in the Xihu Depression through cluster analysis.**(B)** Component matrix of parameters; and **(C)** classification of crude oil samples in the Xihu Depression through principal component analysis. Notes: P, phenanthrene; DMP, dimethylphenanthrene; TMN, trimethylnaphthalene; Diterp, diterpanes; noriP, 4β(H)-19-norisopimarane; iP, isopimarane; Ret, retene; Phy, 16β(H)-phyllocladane; Dri, 8β(H)-drimane; homoDri, 8β(H)-homodrimane; diaDri, diadrimane.

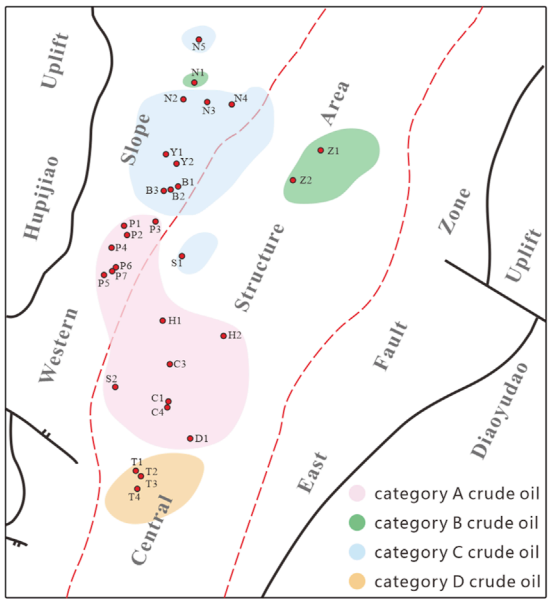

FIGURE 12
Iconography of the distribution of different categories of crude oil in the Xihu Depression. Red dots represent the location of each well.

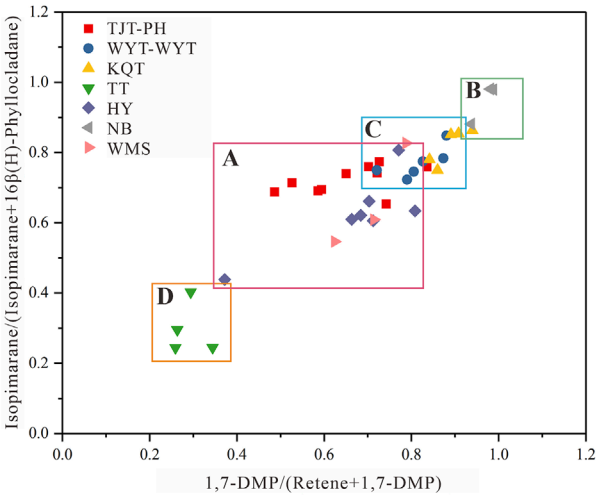

FIGURE 13
Plot of diterpane parameter versus aromatic parameter showing the source input of crude oil from gymnosperms and ferns. Notes: DMP, dimethylphenanthrene.

Cluster analysis is a powerful statistical tool that can elucidate the relationships among various samples by grouping them based on their similarities. In the current study, a set of twelve parameters were selected as variables to analyze a total of forty-one samples. Employing Ward's hierarchical clustering method with squared Euclidean distance as the similarity measure and setting a threshold distance of ten for cluster distinction, this study categorized the forty-one samples into four groups. Category A1 comprises all samples from the HY structural belt and TJT-PH region, in addition to two samples from well S2 within the southern sector of the WMS. Category B1 includes samples from the NB structural belt and the crude oil from well N1. Category C1 contains samples from the WYT-BYT and KQT areas, alongside crude oil from well S1 in the WMS central zone. Category D1 consists of samples from the TT structural belt, as delineated in Figure 11A. Among them, the difference between category B and C samples is relatively small, while category D1 stands out with substantial variations when compared to Categories A1, B1, and C1. The findings from the cluster analysis reveal pronounced regional distinctions in the crude oil geochemical characteristics within the Xihu Depression.

Principal Component Analysis (PCA) is a widely utilized multivariate statistical analysis technique. It simplifies the complexity of multiple observable variables by reducing their dimensionality, thereby encapsulating multi-dimensional information with fewer metrics and uncovering the intrinsic factors that govern the variability of the original variables. In this study, we select the aforementioned parameters as variables for PCA. Through this analysis, the parameters were successfully extracted into two principal components, PC1 and PC2, which together account for a cumulative explained variance of 73.6%. The principal component scores of crude oil samples from the Xihu Depression predominantly fall into four categories: Category A2 crude oil, characterized by scores of both principal component 1(PC1) and principal component 2(PC2) being close to the origin, indicating that all parameters are near the average. Category B2 crude oil, distinguished by lower scores on both PC1 and PC2, indicative of heavier $\delta^{13}C_{oil}$ in the crude oil and a higher ratio of diadrimane/8β(H)-drimane. Category C2 crude oil, which exhibits a lower score for PC1 and a higher score for PC2, marked by elevated levels of diterpanes/nC_{20} and 1,7-DMP/phenanthrene. Category D2 crude oil, identified by high scores for PC1 and lower scores for PC2, characterized by significant ratios of Pr/nC_{17}, Ph/nC_{18}, Pr/Ph, and 16β(H)-phyllocladane/isopimarane (Figure 11B). Figure 11C illustrates the pronounced regional variations in the geochemical characteristics of crude oil from the Xihu Depression. Furthermore, the results of the PCA and cluster analysis demonstrate a high degree of similarity.

In conclusion, the application of multivariate statistical analysis to biomarker compound characteristics in crude oil from the Xihu Depression enables a preliminary classification into four distinct categories: A, B, C, and D. Category A comprises crude oils from the TJT-PH region, and the WMS and HY structural zones. Category B includes the condensate oils from well N1 within the KQT region as well as crude oils from the NB structural zone. Category C is defined by crude oils originating from both the KQT and WYT-BYT regions. Finally, Category D encompasses crude oils from the TT structural zone (Figure 12).

5.2 Organic matter precursors for different crude oil categories

Utilizing the biomarker compounds parameters, multivariate statistical analysis categorizes crude oils from the Xihu Depression into four distinct groups. These biomarker compound parameters

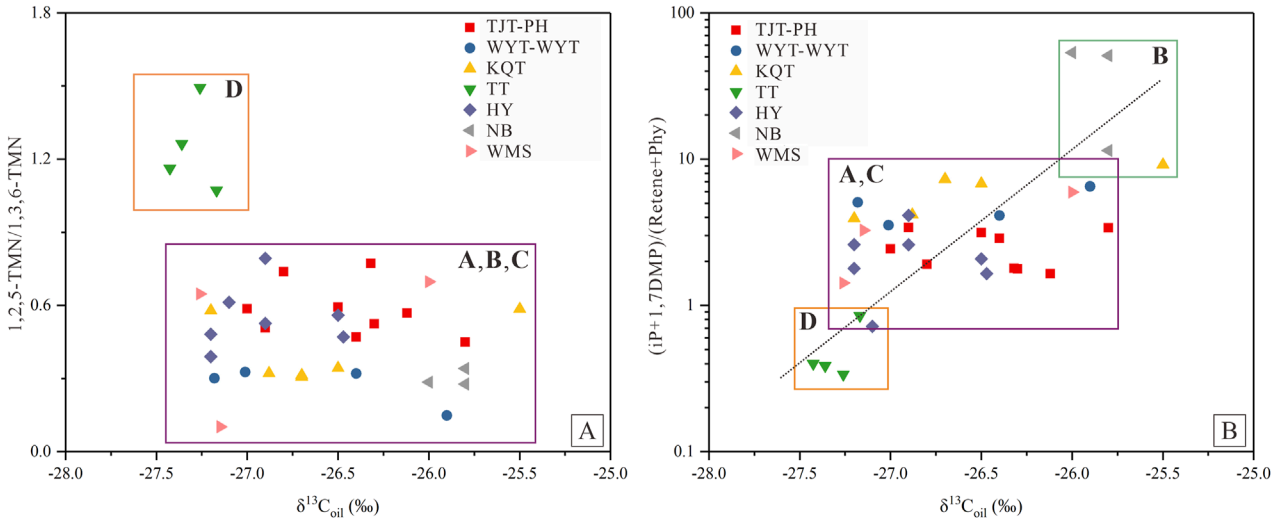

FIGURE 14
(A) Correlation between angiosperm source input and stable carbon isotope ratio, category D crude oil differs from other crude oil. **(B)** Correlation between gymnosperm source input and stable carbon isotope ratio. Notes: TMN-trimethylnaphthalene; DMP, dimethylphenanthrene; iP, isopimarane.

effectively trace the origins of various higher plant classes within the organic matter and their contributions. This insight elucidates the underlying causes of regional variations in the geochemical characteristics of crude oils from the Xihu Depression.

Biomarker compounds serve as microscopic indicators of the organic matter source in crude oil. The remnants of three plant classes—angiosperms, gymnosperms, and ferns—can each transform into distinctive biomarker compounds following sedimentary burial. Olean-18-ene, oleanane, and aromatized compounds such as 1,2,5-TMN, 1,2,5,6-TeMN, and 1-ethyl-2,5-DMN are characteristically derived from angiosperms (Nakamura et al., 2010; Diefendorf et al., 2014). Pimarane, isopimarane, and their aromatized derivatives like 1,7-DMP and 1-ethyl-7-MP predominantly stem from tall coniferous gymnosperms (Otto and Wilde, 2001; Menor-Salván et al., 2010; Pereira et al., 2020). The phyllocladane series compounds and their aromatized counterparts, including 1-methylphenanthrene and retene, exhibit a distinct association with ferns (Kashirtsev et al., 2010; Romero-Sarmiento et al., 2011; Izart et al., 2015).

The preceding section examined the ratios of 1,2,5-TMN/1,3,6-TMN and (1,2,5,6-TeMN+1,2,3,5-TeMN)/∑TeMNs. These ratios are indicative of angiosperm input and exhibit minimal variation across crude oils from the KQT, WYT-BYT, TJT-PH, NB, and HY structural zones. In contrast, the TT structural zone shows a significantly elevated angiosperm input. This observation implies that Category A, B, and C crude oils exhibit a moderate angiosperm contribution, while Category D crude oils are characterized by a more pronounced angiosperm presence.

Diterpanes and their aromatized compounds serve as biomarkers for gymnosperm and fern contributions. Nonetheless, their concentrations markedly diminish in crude oils exhibiting high maturity (Damsté et al., 1986; Peters et al., 2005; Patra et al., 2018). To mitigate the impact of maturity discrepancies, this investigation utilized compound ratios to establish two proxies: isopimarane/(isopimarane+16β(H) phyllocladane) and 1,7-DMP/(retene+1,7-DMP).

As depicted in Figure 13, a good linear correlation exists between these two parameters, with clear differentiation discernible among crude oils of varying categories. Utilizing comprehensive GC-MS analysis, we examined the attributes of aliphatic hydrocarbons and aromatic compounds in crude oils on a consistent scale, thereby formulating an indicator: (isopimarane+1,7-DMP)/(16β(H) phyllocladane + retene). This indicator is designed to offer a more comprehensive representation of the botanical origin of organic matter in crude oils from the study region. Consistent with prior discussion, a higher ratio signifies a greater contribution of gymnosperms, whereas a lower ratio implies a more substantial input of ferns. For category A crude oils, this ratio spans from 0.71 to 4.13; for category B crude oils, it extends from 9.15 to 53.46; for category C crude oils, it varies from 3.12 to 7.31; and for category D crude oils, it fluctuates between 0.34 and 0.85.

Based on the analysis of biomarker compounds associated with angiosperms, gymnosperms, ferns, and other aquatic plants like algae, we can deduce the botanical origins of the organic matter in various types of crude oils from the Xihu Depression. Category A crude oils exhibit a higher contribution from ferns, moderate contributions from gymnosperms and angiosperms, and negligible algal contributions. Category B and Category C crude oils show a higher contribution from gymnosperms, moderate contributions from angiosperms, lower contributions from ferns, and no algal contributions. Category D crude oils are primarily influenced by fern and angiosperm contributions, with minor inputs from aquatic plankton and limited contributions from gymnosperms. These may stem from different hydrocarbon-generating sags than those of Categories A, B, and C. Additionally, the characteristics of the crude oil from well DQ-1 in the southern part of the category A region bear some resemblances to those of Category D crude oils, indicating

that the crude oil from well DQ-1 might be a mixed-source oil from Categories A and D.

Biomarker parameters provide insights into the detailed characteristics of crude oil, while the $\delta^{13}C_{oil}$ encapsulates its overall features. By correlating parameters that indicate the source input from angiosperms and gymnosperms in crude oil with the $\delta^{13}C_{oil}$, it becomes evident that the 1,2,5-trimethylnaphthalene/1,3,6-trimethylnaphthalene ratio, reflecting angiosperm input, does not exhibit a strong correlation with $\delta^{13}C_{oil}$, except for Category D crude oil, which significantly differs from the other three categories (Figure 14). Conversely, the (isopimarane+1,7-DMP)/(16β(H) phyllocladane+retene), indicative of gymnosperm input, demonstrates a robust positive correlation with $\delta^{13}C_{oil}$ (Figure 14), with a pattern of Category D crude oil < Category A crude oil < Category C crude oil < Category B crude oil. Consequently, the input of gymnosperms predominantly shapes the overall profile of the crude oil, and the hydrogen-rich resin derived from gymnosperm conifers plays a pivotal role in the composition of crude oil in the Xihu Depression.

6 Conclusion

This study provides a comprehensive analysis of the crude oil from the Xihu Depression, offering significant insights into its source, depositional environment, and paleoclimatic conditions. Our findings highlight the predominance of terrestrial higher plant inputs, particularly gymnosperms, under oxidative conditions.

Differentiating the crude oil sources into four distinct categories, each characterized by specific plant contributions, underscores the complex interactions between ancient structural formations and paleoclimatic regimes. This enhanced understanding provides a more detailed framework for interpreting the geochemical signatures of crude oils in similar geological settings worldwide.

A key contribution of this work is the proposal of the (isopimarane+1,7-DMP)/(16β(H)-phyllocladane+retene) ratio. Within our dataset, this index shows potential as a supplementary geochemical tool for assessing variations in higher plant, particularly gymnosperm-derived, organic matter input, showing correlations with bulk carbon isotopic compositions.

To further refine the understanding of organic matter provenance and paleoenvironmental reconstructions in the Xihu Depression, future research employing compound-specific isotope analysis on specific biomarkers, such as diterpanes and their aromatized derivatives, is recommended. Such analyses could provide direct isotopic links between biomarkers and their biological precursors, potentially resolving ambiguities in source apportionment derived solely from molecular ratios and enabling a more precise reconstruction of past vegetation patterns and paleoclimatic conditions within the basin.

Data availability statement

The original contributions presented in the study are included in the article/Supplementary Material, further inquiries can be directed to the corresponding author.

Author contributions

JY: Writing – original draft, Conceptualization, Funding acquisition, Investigation, Validation, Visualization, Data curation. GR: Data curation, Formal Analysis, Methodology, Validation, Visualization, Writing – review and editing. HD: Conceptualization, Funding acquisition, Project administration, Resources, Supervision, Writing – review and editing. CX: Investigation, Methodology, Project administration, Supervision, Writing – review and editing.

Funding

The author(s) declare that financial support was received for the research and/or publication of this article. This work was financially supported by the National Natural Science Foundation of China (Grant No. UU2244222) and Guangzhou Science and Technology Program (Grant No. 2023A04J0236).

Acknowledgments

The authors gratefully acknowledge the Shanghai Branch of China National Offshore Oil Corporation (CNOOC) for samples and data collection.

Conflict of interest

The authors declare that the research was conducted in the absence of any commercial or financial relationships that could be construed as a potential conflict of interest.

Generative AI statement

The author(s) declare that no Generative AI was used in the creation of this manuscript.

Publisher's note

Supplementary material

The Supplementary Material for this article can be found online at: https://www.frontiersin.org/articles/10.3389/feart.2025.1627767/full#supplementary-material

References

Abbas, A., Zhu, H., Zeng, Z., and Zhou, X. (2018). Sedimentary facies analysis using sequence stratigraphy and seismic sedimentology in the paleogene Pinghu Formation, Xihu depression, east China sea shelf basin. *Mar. Pet. Geol.* 93, 287–297. doi:10.1016/j.marpetgeo.2018.03.017

Abbassi, S., Edwards, D. S., George, S. C., Volk, H., Mahlstedt, N., Di Primio, R., et al. (2016). Petroleum potential and kinetic models for hydrocarbon generation from the upper cretaceous to paleogene Latrobe group coals and shales in the Gippsland basin, Australia. *Org. Geochem.* 91, 54–67. doi:10.1016/j.orggeochem.2015.11.001

Akinlua, A., Ajayi, T. R., and Adeleke, B. B. (2006). Niger Delta oil geochemistry: insight from light hydrocarbons. *J. Pet. Sci. Eng.* 50, 308–314. doi:10.1016/j.petrol.2005.12.003

Alexander, R., Kagi, R. I., Rowland, S. J., Sheppard, P. N., and Chirila, T. V. (1985). The effects of thermal maturity on distributions of dimethylnaphthalenes and trimethylnaphthalenes in some ancient sediments and petroleums. *Geochim. Cosmochim. Acta* 49, 385–395. doi:10.1016/0016-7037(85)90031-6

Ayinla, H. A., Abdullah, W. H., Makeen, Y. M., Abubakar, M. B., Jauro, A., Yandoka, B. M. S., et al. (2017). Source rock characteristics, depositional setting and hydrocarbon generation potential of Cretaceous coals and organic rich mudstones from Gombe Formation, Gongola Sub-basin, Northern Benue Trough, NE Nigeria. *Int. J. Coal Geol.* 173, 212–226. doi:10.1016/j.coal.2017.02.011

Baset, Z. H., Pancirov, R. J., and Ashe, T. R. (1980). Organic compounds in coal: structure and origins. *Phys. Chem. Earth* 12, 619–630. doi:10.1016/0079-1946(79)90143-5

Budzinski, H., Garrigues, P. H., Connan, J., Devillers, J., Domine, D., Radke, M., et al. (1995). Alkylated phenanthrene distributions as maturity and origin indicators in crude oils and rock extracts. *Geochim. Cosmochim. Acta* 59, 2043–2056. doi:10.1016/0016-7037(95)00125-5

Cai, Z., Wu, N., Yang, H., Gu, Q., and Han, J. (2009). Mechanism of evaporative fractionation in condensate gas reservoirs in Lunnan low salient. *Nat. Gas. Ind.* 29, 21–24. doi:10.3787/j.issn.1000-0976.2009.04.005

Cao, Q., Song, Z., Zhou, X., Liang, S., and Wang, L. (2019). Geochemical characteristics and source of crude oil in Xihu sag, East China Sea Shelf basin. *Petroleum Geol. Exp.* 2, 251–259. doi:10.11781/sysydz201902251

Cheng, X., Hou, D., Zhao, Z., Chen, X., and Diao, H. (2019). Sources of natural Gases in the Xihu sag, East China Sea Basin: insights from stable carbon isotopes and confined system pyrolysis. *Energy fuels.* 33, 2166–2175. doi:10.1021/acs.energyfuels.9b00090

Cheng, X., Hou, D., Zhao, Z., Jiang, Y., Zhou, X., and Diao, H. (2020a). Higher landplant–derived biomarkers in light oils and condensates from the coal-bearing Eocene Pinghu Formation, Xihu sag, East China Sea Shelf Basin. *J. Pet. Geol.* 43, 437–451. doi:10.1111/jpg.12774

Cheng, X., Hou, D., Zhou, X., Liu, J., Diao, H., Jiang, Y., et al. (2020b). Organic geochemistry and kinetics for natural gas generation from mudstone and coal in the Xihu Sag, East China Sea Shelf Basin, China. *Mar. Pet. Geol.* 118, 104405. doi:10.1016/j.marpetgeo.2020.104405

Damsté, J. S., Ten Haven, H. L., De Leeuw, J. W., and Schenck, P. A. (1986). Organic geochemical studies of a Messinian evaporitic basin, northern Apennines (Italy)—II Isoprenoid and *n*-alkyl thiophenes and thiolanes. *Org. Geochem.* 10, 791–805. doi:10.1016/s0146-6380(86)80016-x

Diefendorf, A. F., Freeman, K. H., and Wing, S. L. (2014). A comparison of terpenoid and leaf fossil vegetation proxies in Paleocene and Eocene Bighorn Basin sediments. *Org. Geochem.* 71, 30–42. doi:10.1016/j.orggeochem.2014.04.004

Ding, W., Hou, D., Gan, J., Zhang, Z., and George, S. C. (2022). Aromatic hydrocarbon signatures of the late miocene-early pliocene in the Yinggehai basin, south China sea: implications for climate variations. *Mar. Pet. Geol.* 142, 105733. doi:10.1016/j.marpetgeo.2022.105733

Escobar, M., Márquez, G., Suárez-Ruiz, I., Juliao, T. M., Carruyo, G., and Martínez, M. (2016). Source-rock potential of the lowest coal seams of the marcelina formation at the paso diablo mine in the Venezuelan Guasare basin: evidence for the correlation of amana oils with these Paleocene coals. *Int. J. Coal Geol.* 163, 149–165. doi:10.1016/j.coal.2016.07.003

Fu, N. (1994). Diterpenoid compounds in coal measures and condensates in Xihu sag of East China Sea Basin. *China Offshore Oil Gas. Geol.* 8, 21–28.

García-González, M., Surdam, R. C., and Lee, M. L. (1997). Generation and expulsion of petroleum and gas from almond formation coal, greater Green River basin, Wyoming. *AAPG Bull.* 81, 62–81. doi:10.1306/522b428f-1727-11d7-8645000102c1865d

Gorchs, R., Olivella, M. A., and De Las Heras, F. X. C. (2003). New aromatic biomarkers in sulfur-rich coal. *Org. Geochem.* 34, 1627–1633. doi:10.1016/j.orggeochem.2003.08.002

Hartgers, W. A., Damsté, J. S. S., Requejo, A. G., Allan, J., Hayes, J. M., Ling, Y., et al. (1994). A molecular and carbon isotopic study towards the origin and diagenetic fate of diaromatic carotenoids. *Org. Geochem.* 22, 703–725. doi:10.1016/0146-6380(94)90134-1

He, J., Wang, T., Tang, Y., Zhang, D., Zhang, T., Diao, H., et al. (2023). Geochemical characteristics and gas-washing accumulation mechanism of hydrocarbon from the Xihu sag, east China Sea Basin. *Geoenergy Sci. Eng.* 224, 211639. doi:10.1016/j.geoen.2023.211639

Hou, D., Wang, P., Lin, R., and Li, S. (1992). Distribution of some diterpenoid hydrocarbons in Huangxian brown coal and their thermal evolution. *Acta Pet. Sin.* 13, 27. doi:10.7623/syxb199203005

Izart, A., Suarez-Ruiz, I., and Bailey, J. (2015). Paleoclimate reconstruction from petrography and biomarker geochemistry from Permian humic coals in Sydney Coal Basin (Australia). *Int. J. Coal Geol.* 138, 145–157. doi:10.1016/j.coal.2014.12.009

Jauro, A., Obaje, N. G., Agho, M. O., Abubakar, M. B., and Tukur, A. (2007). Organic geochemistry of cretaceous lamza and chikila coals, upper benue trough, Nigeria. *Fuel* 86, 520–532. doi:10.1016/j.fuel.2006.07.031

Jiang, Y., Hou, D., Diao, H., and Cheng, X. (2020). Characteristics and indication of terrestrial biomarkers of crude oil in different local structures of Xihu Depression,East China Sea Basin. *Bull. Geol. Sci. Technol.* 39 (03), 89–98. doi:10.19509/j.cnki.dzkq.2020.0310

Kang, S., Shao, L., Qin, L., Li, S., Liu, J., Shen, W., et al. (2020). Hydrocarbon generation potential and depositional setting of Eocene oil-prone coaly source rocks in the Xihu sag, east China Sea Shelf basin. *ACS Omega* 5, 32267–32285. doi:10.1021/acsomega.0c04109

Kashirtsev, V. A., Moskvin, V. I., Fomin, A. N., and Chalaya, O. N. (2010). Terpanes and steranes in coals of different genetic types in Siberia. *Russ. Geol. Geophys.* 51, 404–411. doi:10.1016/j.rgg.2010.03.007

Le Metayer, P., Grice, K., Chow, C. N., Caccetta, L., Maslen, E., Dawson, D., et al. (2014). The effect of origin and genetic processes of low molecular weight aromatic hydrocarbons in petroleum on their stable carbon isotopic compositions. *Org. Geochem.* 72, 23–33. doi:10.1016/j.orggeochem.2014.04.008

Li, W., Chen, J., Liu, K., Fu, R., Chen, C., Wang, Y., et al. (2023). Studies on the source and phase characteristics of oil and gas: evidence from hydrocarbon geochemistry in the pingbei area of Xihu sag, the East China Sea Shelf basin, China. *Energies* 16, 6529. doi:10.3390/en16186529

Losh, S., Cathles, L., and Meulbroek, P. (2002). Gas washing of oil along a regional transect, offshore Louisiana. *Org. Geochem.* 33, 655–663. doi:10.1016/s0146-6380(02)00025-6

Menor-Salván, C., Najarro, M., Velasco, F., Rosales, I., Tornos, F., and Simoneit, B. R. (2010). Terpenoids in extracts of lower cretaceous ambers from the Basque-Cantabrian Basin (El Soplao, Cantabria, Spain): paleochemotaxonomic aspects. *Org. Geochem.* 41, 1089–1103. doi:10.1016/j.orggeochem.2010.06.013

Nakamura, H., Sawada, K., and Takahashi, M. (2010). Aliphatic and aromatic terpenoid biomarkers in Cretaceous and Paleogene angiosperm fossils from Japan. *Org. Geochem.* 41, 975–980. doi:10.1016/j.orggeochem.2010.03.007

Obaje, N. G., and Hamza, H. (2000). Liquid hydrocarbon source-rock potential of mid-Cretaceous coals and coal measures in the Middle Benue Trough of Nigeria. *Int. J. Earth Sci. Geol. Rundsch.* 89, 130–139. doi:10.1007/s005310050321

Otto, A., and Wilde, V. (2001). Sesqui-di-and triterpenoids as chemosystematic markers in extant conifers—a review. *Bot. Rev.* 67, 141–238. doi:10.1007/bf02858076

Patra, S., Dirghangi, S. S., Rudra, A., Dutta, S., Ghosh, S., Varma, A. K., et al. (2018). Effects of thermal maturity on biomarker distributions in gondwana coals from the satpura and damodar valley basins, India. *Int. J. Coal Geol.* 196, 63–81. doi:10.1016/j.coal.2018.07.002

Pereira, R., de Lima, F. J., Simbras, F. M., Bittar, S. M. B., Kellner, A. W. A., Saraiva, A. Á. F., et al. (2020). Biomarker signatures of cretaceous gondwana amber from ipubi formation (araripe basin, Brazil) and their palaeobotanical significance. *J. S. Am. Earth Sci.* 98, 102413. doi:10.1016/j.jsames.2019.102413

Peters, K. E., Walters, C. C., and Moldowan, J. M. (2005). *The biomarker guide*. Cambridge University Press.

Qin, J., Yang, Z., Liang, W., and Zeng, F. (1998). High-resolution sequence stratigraphy of the Holocene strata on the East China Sea shelf. *Sediment. Facies Palaeogeogr.* 18, 11–26.

Quan, Y., Chen, Z., Jiang, Y., Diao, H., Xie, X., Lu, Y., et al. (2022). Hydrocarbon generation potential, geochemical characteristics, and accumulation contribution of coal-bearing source rocks in the Xihu Sag, East China Sea Shelf Basin. *Mar. Pet. Geol.* 136, 105465. doi:10.1016/j.marpetgeo.2021.105465

Radke, M., Welte, D. H., and Willsch, H. (1991). Distribution of alkylated aromatic hydrocarbons and dibenzothiophenes in rocks of the Upper Rhine Graben. *Chem. Geol.* 93, 325–341. doi:10.1016/0009-2541(91)90122-8

Romero-Sarmiento, M. F., Riboulleau, A., Vecoli, M., Laggoun Défarge, F., and Versteegh, G. J. (2011). Aliphatic and aromatic biomarkers from carboniferous coal deposits at dunbar (east Lothian, Scotland): palaeobotanical and palaeoenvironmental significance. *Palaeogeogr. Palaeoclimatol. Palaeoecol.* 309, 309–326. doi:10.1016/j.palaeo.2011.06.015

Shen, Y., Qin, Y., Guo, Y., Zhao, Z., Yuan, X., Qu, Z., et al. (2016). Development characteristics of coal-measure source rocks divided on the basis of Milankovich coal accumulation cycle in Pinghu Formation, Xihu sag. *Acta Pet. Sin.* 37, 706. doi:10.7623/syxb201606002

Su, A., Chen, H., Lei, M., Li, Q., and Wang, C. (2019). Paleo-pressure evolution and its origin in the Pinghu slope belt of the Xihu Depression, East China Sea Basin. *Mar. Pet. Geol.* 107, 198–213. doi:10.1016/j.marpetgeo.2019.05.017

Su, A., Chen, H., Wang, C., Li, P., Zhang, H., Xiong, W., et al. (2013). Genesis and maturity identification of oil and gas in the Xihu sag, East China Sea Basin. *Pet. Explor. Dev.* 40, 558–565. doi:10.1016/s1876-3804(13)60073-7

Thompson, K. F. M. (1988). Gas-condensate migration and oil fractionation in deltaic systems. *Mar. Pet. Geol.* 5, 237–246. doi:10.1016/0264-8172(88)90004-9

Wang, W., Lin, C., Zhang, X., Dong, C., Ren, L., and Lin, J. (2020). Effect of burial history on diagenetic and reservoir-forming process of the Oligocene sandstone in Xihu sag, East China Sea Basin. *Mar. Pet. Geol.* 112, 104034. doi:10.1016/j.marpetgeo.2019.104034

Wang, Y., Chen, J., Pang, X., Zhang, T., Zhu, X., and Liu, K. (2022). Hydrocarbon generation and expulsion of tertiary coaly source rocks and hydrocarbon accumulation in the Xihu Sag of the East China Sea Shelf Basin, China. *J. Asian Earth Sci.* 229, 105170. doi:10.1016/j.jseaes.2022.105170

Wang, Y., Qin, Y., Yang, L., Liu, S., Elsworth, D., and Zhang, R. (2020). Organic geochemical and petrographic characteristics of the coal measure source rocks of Pinghu Formation in the Xihu sag of the East China Sea Shelf basin: implications for coal measure gas potential. *Acta Geol. Sin. Eng.* 94, 364–375. doi:10.1111/1755-6724.14303

Wei, H. (2013). Analysis of main controlling factors and mechanism for condensate gas–oil accumulation in Xihu depression. Ph.D. Thesis. Beijing: China University of Petroleum.

Wu, Z. (2014). Cenozoic biostratigraphy of the Xihu Sag, northeast continental shelf basin of the East China Sea. *J. Stratigr.* 38, 470–478. doi:10.19839/i.cnki.dcxzz.2014.04.012

Wu, Z., Grohmann, S., and Littke, R. (2024). Geochemistry and petrology of Early Permian lacustrine shales in the Lodève Basin, Southern France: depositional history, organic matter accumulation and thermal maturity. *Int. J. Coal Geol.* 284, 104469. doi:10.1016/j.coal.2024.104469

Xie, G., Shen, Y., Liu, S., and Hao, W. (2018). Trace and rare earth element (REE) characteristics of mudstones from Eocene Pinghu Formation and Oligocene Huagang Formation in Xihu sag, East China Sea Basin: implications for provenance, depositional conditions and paleoclimate. *Mar. Pet. Geol.* 92, 20–36. doi:10.1016/j.marpetgeo.2018.02.019

Xu, H., Hou, D., Cao, B., Chen, X., and Xu, T. (2016). Geochemical characteristics of high-maturity crude oils in the Xihu Depression, East China Sea Basin. *Geochem. J.* 50, 163–178. doi:10.2343/geochemj.2.0402

Xu, T., Hou, D., and Cao, B. (2015). Study of precursors for condensates and light oils in Xihu sag of east China Sea Basin. *Geochimica* 44, 289–300. doi:10.19700/j.0379-1726.2015.03.008

Yang, F., Xu, X., Zhao, W., and Sun, Z. (2011). Petroleum accumulations and inversion structures in the Xihu depression, east China Sea Basin. *J. Pet. Geol.* 34, 429–440. doi:10.1111/j.1747-5457.2011.00513.x

Yang, Y., Xie, X., Li, Y., Guo, G., Xi, X., and Ding, W. (2023). Formation and distribution of coal measure source rocks in the Eocene Pinghu Formation in the Pinghu slope of the Xihu Depression, East China Sea Shelf basin. *Acta Oceanol. Sin.* 42, 254–269. doi:10.1007/s13131-023-2176-8

Ye, J., Qing, H., Bend, S. L., and Gu, H. (2007). Petroleum systems in the offshore Xihu basin on the continental shelf of the East China sea. *AAPG Bull.* 91, 1167–1188. doi:10.1306/02220705158

Zhan, Z., Wang, G., Tian, Y., Zhan, X., Liang, T., Wang, Y., et al. (2023). Determination and petroleum geochemical significance of short-chain alkylbenzenes in lacustrine source rocks. *Org. Geochem.* 185, 104685. doi:10.1016/j.orggeochem.2023.104685

Zhang, G., Jin, L., Lan, L., and Zhao, Z. (2015). Analysis of the orderly distribution of oil and gas fields in China based on the theory of co-control of source and heat. *Nat. Gas. Ind. B* 2, 49–76. doi:10.1016/j.ngib.2015.02.005

Zhang, S., and Jiang, Y. (2013). High resolution sequence stratigraphy of the Eocene Pinghu Formation, Pinghu slope, Xihu sag. *Mar. Geol. Front.* 29, 8–13. doi:10.16028/j.1009-2722.2013.10.011

Zhang, W., and Zhang, M. (2012). Biomarker characteristics of saturated hydrocarbon in typical marine oils and typical coal-formed oils. *J. Oil Gas. Technol.* 34, 25–28. doi:10.3969/j.issn.1000-9752.2012.06.006

Zhao, X., Chen, J., Guo, W., Shi, S., Zhang, C., Chen, J., et al. (2013). Geochemical characteristics of aromatic hydrocarbon in crude oil and source rocks from Nai 1 block of Naiman depression, Kailu Basin. *Geochimica* 42, 262–273. doi:10.3969/j.issn.0379-1726.2013.03.007

Zhao, Z., Wang, P., Qi, P., and Guo, R. (2016). Regional background and tectonic evolution of east China Sea Basin. *Earth Sci.* 41, 546–554. doi:10.3799/dqkx.2016.045

Zhou, X. (2020). Geological understanding and innovation in Xihu sag and breakthroughs in oil and gas exploration. *China Offshore Oil Gas.* 32, 1–12. doi:10.11935/j.issn.1673-1506.2020.01.00

Zhu, X., Chen, J., Li, W., Pei, L., Liu, K., Chen, X., et al. (2020). Hydrocarbon generation potential of Paleogene coals and organic rich mudstones in Xihu sag, East China Sea Shelf basin, offshore eastern China. *J. Pet. Sci. Eng.* 184, 106450. doi:10.1016/j.petrol.2019.106450

Zhu, X., Chen, J., Zhang, C., Wang, Y., Liu, K., and Zhang, T. (2021). Effects of evaporative fractionation on diamondoid hydrocarbons in condensates from the Xihu sag, East China Sea Shelf basin. *Mar. Pet. Geol.* 126, 104929. doi:10.1016/j.marpetgeo.2021.104929

Zhu, Y., Li, Y., Zhou, J., and Gu, S. (2012). Geochemical characteristics of Tertiary coal-bearing source rocks in Xihu depression, East China Sea basin. *Mar. Pet. Geol.* 35, 154–165. doi:10.1016/j.marpetgeo.2012.01.005